


RESEARCH

Open Access



HGF-mediated elevation of ETV1 facilitates hepatocellular carcinoma metastasis through upregulating PTK2 and c-MET

Tongyue Zhang^{1†}, Yijun Wang^{1†}, Meng Xie^{1†}, Xiaoyu Ji¹, Xiangyuan Luo¹, Xiaoping Chen², Bixiang Zhang², Danfei Liu¹, Yangyang Feng¹, Mengyu Sun¹, Wenjie Huang^{2,3*} and Limin Xia^{1*} 

Abstract

Background: Metastasis is a major determinant of death in patients with hepatocellular carcinoma (HCC). Dissecting key molecular mediators that promote this malignant feature may help yield novel therapeutic insights. Here, we investigated the role of E-twenty-six transformation-specific variant 1 (ETV1), a member of the E-twenty-six transformation-specific (ETS) family, in HCC metastasis.

Methods: The clinical significance of ETV1 and its target genes in two independent cohorts of HCC patients who underwent curative resection were assessed by Kaplan–Meier analysis and Multivariate Cox proportional hazards model. Luciferase reporter assay and chromatin immunoprecipitation assay were used to detect the transcriptional regulation of target gene promoters by ETV1. The effect of ETV1 on invasiveness and metastasis of HCC were detected by transwell assays and the orthotopically metastatic model.

Results: ETV1 expression was frequently elevated in human HCC specimens. Increased ETV1 expression was associated with the malignant biological characteristics and poor prognosis of HCC patients. ETV1 facilitated invasion and metastasis of HCC cells in vitro and in vivo. Mechanistically, ETV1 promoted HCC metastasis via upregulating metastasis-related genes, including *protein tyrosine kinase 2 (PTK2)* and *MET*. Down-regulated the expression of PTK2 or tyrosine protein kinase Met (c-MET) decreased ETV1-mediated HCC metastasis. Hepatocyte growth factor (HGF) upregulated ETV1 expression through activating c-MET-ERK1/2-ELK1 pathway. Notably, in two independent cohorts, patients with positive coexpression of ETV1/PTK2 or ETV1/c-MET had worse prognosis. Furthermore, the combination of PTK2 inhibitor defactinib and c-MET inhibitor capmatinib significantly suppressed HCC metastasis induced by ETV1.

[†]Tongyue Zhang, Yijun Wang and Meng Xie contributed equally to this work.

*Correspondence: huangwenjie@tjh.tjmu.edu.cn; xialimin@tjh.tjmu.edu.cn

¹ Department of Gastroenterology, Institute of Liver and Gastrointestinal Diseases, Hubei Key Laboratory of Hepato-Pancreato-Biliary Diseases, Tongji Hospital of Tongji Medical College, Huazhong University of Science and Technology, Wuhan 430030, Hubei Province, China

² Hepatic Surgery Center, Hubei Key Laboratory of Hepato-Pancreato-Biliary Diseases, Tongji Hospital of Tongji Medical College, Huazhong University of Science and Technology, Wuhan 430030, Hubei Province, China

Full list of author information is available at the end of the article



Conclusion: This study uncovers functional and prognostic roles for ETV1 in HCC and exposes a positive feedback loop of HGF-ERK1/2-ETV1-c-MET. Targeting this pathway may provide a potential therapeutic intervention for ETV1-overexpressing HCC.

Keywords: E-twenty-six transformation-specific variant 1, Tyrosine protein kinase Met, Protein tyrosine kinase 2, Defactinib, Capmatinib

Background

Hepatocellular carcinoma (HCC) ranks the third leading cause of cancer-related deaths around the world [1]. Metastasis and recurrence often lead to the deaths of HCC patients [2, 3]. Despite the diagnostic methods and treatments have been a step forward after decades of efforts, only a minority of unselected patients benefit [4]. Due to the complex molecular pathogenesis and the lack of appropriate biomarkers, many targeted drugs used as a single agent, such as sorafenib and tivantinib, did not produce ideal clinical benefits [5–7]. To date, the five-year survival rate of advanced HCC is still low [7]. For this reason, attention has been drawn to new combination strategies for better therapeutic efficacy. For example, bevacizumab plus atezolizumab was approved as the first-line treatment for advanced HCC patients for bringing better survival benefits than sorafenib [8–10]. At present, substantial clinical trials involving combination therapy are in progress. Accordingly, it is essential to gain a more thorough comprehension of the molecular mechanism responsible for HCC metastasis and propose potential therapies that are most likely to benefit a certain patient population.

The human E-twenty-six transformation-specific (ETS) family comprises a group of evolutionarily conserved transcription factors, characterized by a highly conserved ETS domain in the C-terminal region recognizing 5'-GGAA/T-3' motif. It has 28 members belonging to 12 separate clusters [11]. ETS factors govern a plethora of developmental and physiological processes, including cell proliferation, differentiation, migration, tissue remodeling, and angiogenesis [11]. ETV1, also named ETS-related protein 81 (ER81), is a member of the polyomavirus enhancer activator 3 (PEA3) subfamily (ETV1, ETV4, ETV5), which is featured with an acidic transactivation domain at the N-terminus [12]. In development, ETV1 performs physiological functions in branching morphogenesis, rapid conduction physiology in the heart and motor coordination [13–15]. Knockout of ETV1 in mice usually leads to motor discoordination and death in the third weeks of birth [15, 16]. ETV1 dysregulation leads to initiation and progression of multiple types of tumors. For example, ETV1 is frequently dysregulated in prostate cancer and reported to be overexpressed in the most aggressive prostate tumors [17]. ETV1 induces cell

migration and invasion of prostate cancer via stabilizing β -catenin and directly binding to MMP1/7 [18, 19]. In pancreatic ductal adenocarcinoma, ETV1 expression is increased in primary and metastatic specimens. It facilitates epithelial-mesenchymal transition (EMT), stromal expansion and metastasis through regulating hyaluronic acid synthase 2 (HAS2) and secreted protein acidic and rich in cysteine (SPARC) in mice [20]. In addition, ETV1 is also known to be required for gastrointestinal stromal tumor initiation and proliferation. It plays as a master regulator in oncogenic transcriptional programme and forms a feedback circuit together with mutant KIT [21]. Nevertheless, the expression and the functional role of ETV1 in HCC remain elusive.

Accumulating data indicate a central role for the hepatocyte growth factor/tyrosine protein kinase Met (HGF/c-Met) pathway in HCC metastasis. Physiologically, the HGF/c-MET axis participates in embryogenesis, cell growth and movement, tissue morphogenesis, morphological differentiation, and organ regeneration [22]. Upon binding to HGF, dimerization and trans-autophosphorylation of c-MET activate various downstream signaling pathways, including the ERK1/2/JNKs/p38 MAPK and the PI3K-Akt pathway, which reach the nucleus to affect gene expression involving angiogenesis and metastasis [22–24]. In HCC, HGF promotes EMT and enhances invasion of HCC cells with increased expression of MMP9 and Snail [25, 26]. In human HCC samples, c-MET expression is associated with intrahepatic metastatic nodules and vascular invasion [27–29]. Patients with HCC and high expression of c-MET were reported to have an early recurrence and poor survival time [28, 30]. Thus, c-MET is considered an intriguing therapeutic target for HCC. However, no selective c-MET inhibitors have been approved for HCC patients, which calls for further study.

This study revealed the clinicopathological significance and function of ETV1 in HCC. Elevated ETV1 expression indicated poor prognosis in HCC and promoted HCC metastasis via upregulating PTK2 and c-MET. HGF/c-MET signaling enhanced ETV1 expression through ERK1/2 activation, which in turn upregulated c-MET expression, forming a positive feedback circuit. Combined treatment of PTK2 inhibitor plus c-MET inhibitor impeded ETV1-induced HCC metastasis.

Methods

Experimental metastasis mouse model

Male 5-week-old BALB/C nude mice were raised under standard conditions. Animal experiments were approved by the Committee on the Tongji Hospital of Tongji Medical College, Huazhong University of Science and Technology. In the orthotopic xenograft model, human fluorescein-labeled 2.0×10^6 HCC cells were resuspended at 50 μ l phosphate-buffered saline and mixed with 50 μ l matrigel injected into the left lobe livers of nude mice (ten per group). Defactinib was orally administered at a dose of 25 mg/kg twice a day, capmatinib was orally administered at a dose of 10 mg/kg/day. The formation of the tumors were detected by bioluminescence. D-luciferin (Perkin-Elmer) was intraperitoneally injected into the mice to detect signals. The bioluminescence images were obtained by the Lago X optical imaging system (SI Imaging). At the predetermined endpoint (9 weeks), the livers and lungs of nude mice were preserved for histological study.

The human liver cancer RT² profiler PCR array

The Human Liver Cancer RT² Profiler PCR Array (Cat. no. 330231 PAHS-133ZA) profiles the expression of 84 key genes involved in the progression of hepatocellular carcinoma (HCC), as well as other forms of hepatocarcinogenesis. This array includes genes commonly up- and down-regulated in HCC, genes involved in commonly altered signal transduction pathways, and genes involved in other dysregulated biological pathways such as epithelial to mesenchymal transition, cell adhesion, apoptosis, and inflammation. PLC/PRF/5-control and PLC/PRF/5-ETV1, MHCC97H-shControl cells and MHCC97H-shETV1 cells were used. RNA extraction, DNase treatment, and RNA cleanup were performed according to the manufacturer's protocol (Qiagen). The cDNA of each group was synthesized using the RT² First Strand Kit (Qiagen). Gene expression profiling of each group was conducted using the Human liver cancer RT² Profiler PCR Array, stored at -20°C . The cDNA synthesis reaction was mixed with $2 \times \text{RT}^2$ qPCR SYBR Green Mastermix and ddH₂O, and then dispensed to the PCR array 96-well plate (25 μ L/well). A 2-step cycling program was performed using the Bio-Rad CFX96. Data normalization was done by correcting all Ct values based on the average Ct values of several housekeeping genes present on array. Each assay was conducted in triplicate.

Immunohistochemistry

First, 4- μ m-thick paraffin tissue sections were baked at 60°C for one hour to deparaffinize and treated with 3% hydrogen peroxide in methanol. After 15 min, the tissue sections were washed with phosphate-buffered saline.

Then the microwave antigen repair was used. Next, sections were incubated overnight at 4°C with the primary antibody. The tissue microarrays were stained for ETV1 (Ruiying, RLT1604), PTK2 (Cell Signaling Technology, #3285), and c-MET (Cell Signaling Technology, #8198). The use of pre-immunized mouse serum was used as the negative control. Slides were incubated with the peroxidase-conjugated second antibody (Santa Cruz) for half an hour and then visualized with diaminobenzidine. Finally, the images were acquired through a light microscope (Olympus, Japan) with a DP70 digital camera.

Agents

PI3K inhibitor LY294002, ERK1/2 inhibitor SCH772984, JNK inhibitor SP600125, p38 inhibitor SB203580, capmatinib and defactinib were purchased from MedChemExpress. The agents were used under the standard protocols. The HCC cells were pretreated with PI3K inhibitor LY294002 (10 μ M), ERK1/2 inhibitor SCH772984 (10 μ M), JNK inhibitor SP600125 (10 μ M), or p38 inhibitor SB203580 (10 μ M) for 1 h. Defactinib was orally administered at a dose of 25 mg/kg twice a day, capmatinib was orally administered at a dose of 10 mg/kg/day. The treatment began on the seventh day after the establishment of the animal model and lasted eight weeks.

Statistical analysis

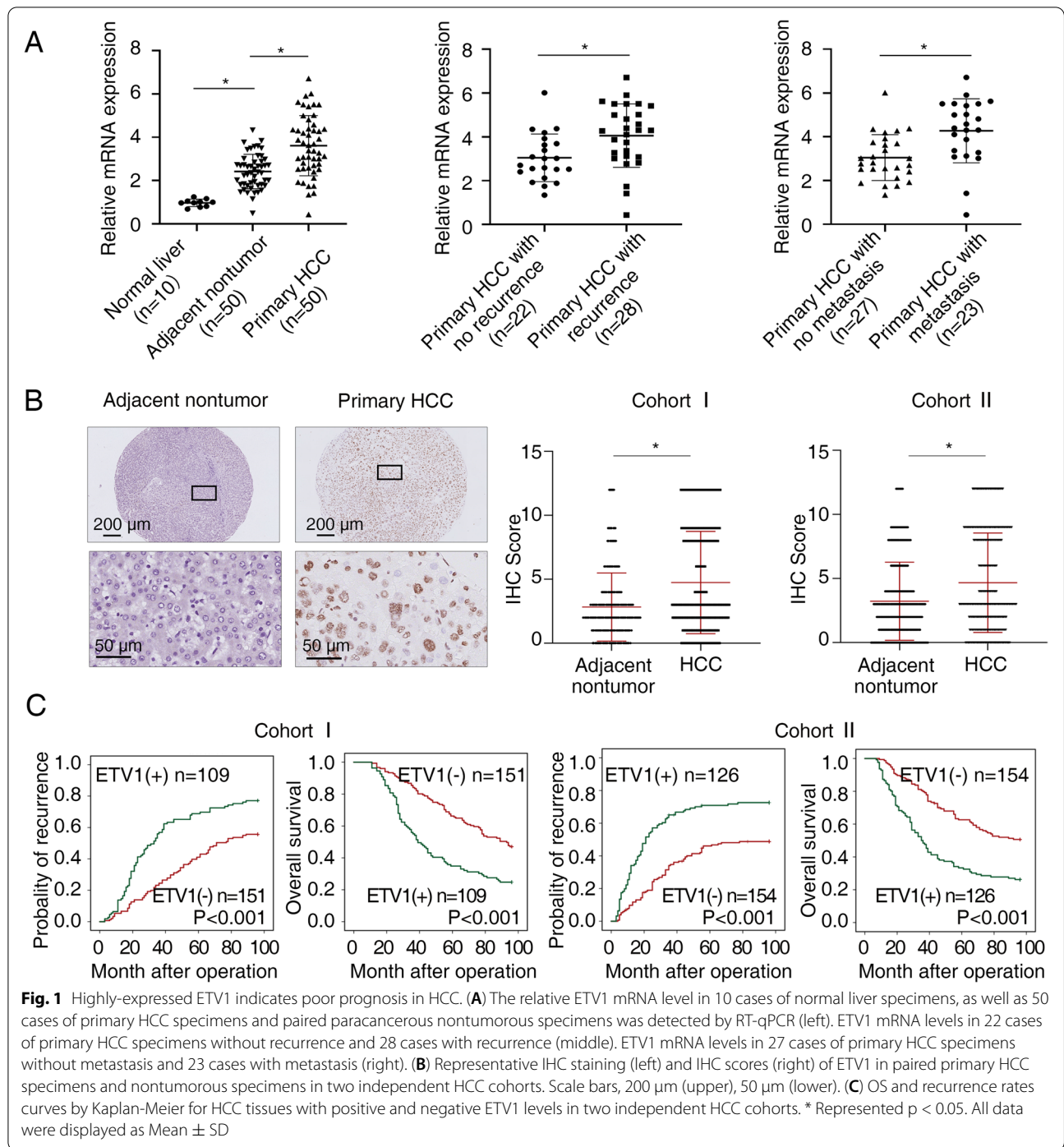
All data were displayed as the mean \pm standard deviation (SD). Student's t-tests, Mann-Whitney U tests, and Wilcoxon signed-rank test were used for comparison between data of two groups with normal distribution, abnormal distribution, and matched pairs, respectively. One-way ANOVA, followed by Tukey's post hoc analysis, was used for comparison among multiple groups. χ^2 test was for categorical data. Kaplan-Meier analysis (log-rank test) was applied to depict the cumulative recurrence rates and overall survival curves. Multivariate analysis was carried out through Cox regression analysis. The SPSS 20.0 software and GraphPad Prism 8.0 were employed for statistical analyses. A value of $p < 0.05$ was considered to be significant.

The exhaustive information of materials and methods were described in the [supplementary materials and methods](#).

Results

Highly-expressed ETV1 indicates poor prognosis in HCC and displays a promoting effect on HCC metastasis

We tested the mRNA level of ETV1 by quantitative RT-PCR (RT-qPCR) in 10 normal liver specimens, as well as 50 matched pairs of adjacent nontumorous and primary HCC specimens. ETV1 was lowly expressed in human



normal liver specimens, which is consistent with a previous report [31]. The mRNA level of ETV1 in primary HCC specimens was higher than that in adjacent nontumorous specimens or normal liver specimens (Fig. 1A left). In addition, as shown in the middle and right parts of Fig. 1A, the ETV1 expression in recurrent or metastatic HCC specimens was higher than those without

recurrence or metastasis. Subsequently, immunohistochemical (IHC) staining was performed to detect ETV1 expression in two independent cohorts (cohort I, $n = 260$; cohort II, $n = 280$) (Fig. 1B). Consistent with the mRNA level, ETV1 protein level in human HCC specimens was higher when compared to paracancerous nontumorous specimens. Particularly, in both cohorts, increased ETV1

Table 1 Correlation between ETV1 expression and clinicopathological characteristics of HCCs in two independent cohorts of human HCC tissues

Clinicopathological variables	Tumor ETV1 expression		P Value	Tumor ETV1 expression		P Value
	Negative (n = 151)	Positive (n = 109)		Negative (n = 154)	Positive (n = 126)	
Age	52.11 (11.915)	51.77 (10.417)	0.411	50.57 (10.053)	51.51 (9.743)	0.351
Sex	female	31	0.428	19	25	0.100
	male	120		135	101	
Serum AFP	≤ 20 ng/ml	46	0.045	32	23	0.652
	> 20 ng/ml	105		122	103	
Virus infection	HBV	108	0.523	119	106	0.406
	HCV	14		11	8	
	HBV + HCV	9		3	4	
	none	20		11	8	
Cirrhosis	absent	40	0.674	42	34	1.000
	present	111		112	92	
Child–pugh score	Class A	113	0.884	130	103	0.630
	Class B	38		24	23	
Tumor number	single	91	0.703	124	86	0.026
	multiple	60		30	40	
Maximal tumor size	≤ 5 cm	69	0.126	102	56	< 0.001
	> 5 cm	82		52	70	
Tumor encapsulation	present	95	0.008	118	77	0.006
	absent	56		36	49	
Microvascular invasion	absent	97	< 0.001	97	56	0.003
	present	54		57	70	
Tumor differentiation	I-II	131	0.001	132	77	< 0.001
	III-IV	20		22	49	
TNM stage	I-II	128	< 0.001	136	82	< 0.001
	III	23		18	44	

expression was significantly correlated with loss of tumor encapsulation, poor tumor differentiation, microvascular invasion, as well as advanced tumor nodular metastasis (TNM) stage (Table 1). As Kaplan–Meier survival analysis illustrated, the high ETV1 level in HCC patients was associated with higher recurrence risks and worse overall survival (OS) compared to low ETV1 expression (Fig. 1C). In concordance with our data, ETV1 was upregulated in tumor tissues, and the high ETV1 mRNA level was correlated with poor survival for patients with HCC in TCGA (Fig. S1A). Notably, multivariate analysis showed that the ETV1 level was an independent risk factor of recurrence and survival in HCC patients (Table 2). Altogether, our data demonstrated that increased ETV1 expression contributed to malignant characteristics of HCC and was associated with a high risk of recurrence and poor survival in HCC patients.

To interrogate the function of ETV1 in HCC, we first assessed the mRNA and protein levels in a panel of HCC cell lines. High endogenous ETV1 expression was

confirmed in multiple HCC cells, especially in those with high metastatic potential (HCCLM3, HCCLM6, and MHCC97H), which suggested its potential role in HCC metastasis (Fig. S1 B-C). We then generated stable PLC/PRF/5-ETV1 cell line and MHCC97H-shETV1 cell line (Fig. 2A). As shown in Fig. 2B, cell migration and invasion, detected by transwell assays, were increased in PLC/PRF/5-ETV1 cells and decreased in MHCC97H-shETV1 cells when compared to their controls. Based on the knockdown effect, the shETV1-3 was chosen for the following studies. Furthermore, cell proliferation, as measured by CCK-8 assay and colony formation assay, was enhanced upon overexpression of ETV1 and vice versa (Fig. S1 D-E).

Next, we examined whether ETV1 is responsible for tumor growth and metastasis in vivo. We performed an orthotopically metastatic model and measured with the bioluminescence imaging (BLI) signals. Compared with PLC/PRF/5-Control group, PLC/PRF/5-ETV1 group demonstrated increased bioluminescence intensity,

Table 2 Univariate and multivariate analysis of factors associated with time to recurrence and overall survival in two independent cohorts of human HCC

Cohort I (N = 260) Clinical Variables	Time To Recurrence		Overall Survival	
	HR(95%CI)	P value	HR(95%CI)	P value
Univariate Analysis				
Age	0.982(0.969–0.995)	0.006	0.981(0.968–0.994)	0.005
Sex (male versus female)	0.925(0.629–1.360)	0.692	0.873(0.593–1.286)	0.492
Serum AFP (> 20 versus ≤ 20 ng/ml)	1.349(0.943–1.931)	0.102	1.405(0.970–2.036)	0.072
HBV infection (yes versus no)	0.792(0.564–1.112)	0.178	0.767(0.543–1.081)	0.130
Cirrhosis (present versus absent)	0.903(0.647–1.259)	0.548	0.876(0.625–1.228)	0.442
Child–pugh score (B versus A)	0.959(0.675–1.364)	0.818	0.948(0.661–1.358)	0.769
Tumor number (multiple versus single)	1.961(1.447–2.656)	< 0.001	2.048(1.503–2.791)	< 0.001
Maximal tumor size (> 5 versus ≤ 5 cm)	1.510(1.103–2.066)	0.010	1.573(1.139–2.173)	0.006
Tumor encapsulation (absent versus present)	3.422(2.507–4.669)	< 0.001	3.584(2.607–4.927)	< 0.001
Microvascular invasion (present versus absent)	3.111(2.280–4.245)	< 0.001	3.315(2.411–4.558)	< 0.001
Tumor differentiation (III- IV versus I-II)	3.155(2.243–4.437)	< 0.001	3.363(2.385–4.743)	< 0.001
TNM stage (III versus I-II)	6.680(4.741–9.414)	< 0.001	7.093(5.015–10.033)	< 0.001
ETV1 (positive versus negative)	2.059(1.519–2.792)	< 0.001	2.143(1.571–2.922)	< 0.001
Multivariate analysis				
Tumor number (multiple versus single)	1.441(0.925–2.247)	0.106	1.530(0.973–2.406)	0.066
Maximal tumor size (> 5 versus ≤ 5 cm)	1.417(0.966–2.078)	0.075	1.465(0.986–2.175)	0.059
Tumor encapsulation (absent versus present)	1.335(0.840–2.121)	0.222	1.289(0.803–2.072)	0.293
Microvascular invasion (present versus absent)	1.663(1.082–2.556)	0.020	1.808(1.168–2.800)	0.008
Tumor differentiation (III- IV versus I-II)	1.569(1.075–2.288)	0.019	1.651(1.131–2.411)	0.009
TNM stage (III versus I-II)	3.004(1.815–4.971)	< 0.001	3.004(1.796–5.026)	< 0.001
ETV1 (positive versus negative)	1.651(1.201–2.269)	0.002	1.748(1.266–2.415)	0.001
Univariate Analysis				
Age	0.992(0.977–1.008)	0.327	0.988(0.972–1.003)	0.117
Sex (male versus female)	1.080(0.695–1.678)	0.732	0.987(0.645–1.510)	0.952
Serum AFP (> 20 versus ≤ 20 ng/ml)	0.951(0.657–1.377)	0.789	0.907(0.631–1.302)	0.595
HBV infection (yes versus no)	2.203(1.380–3.519)	0.001	2.305(1.444–3.679)	< 0.001
Cirrhosis (present versus absent)	1.212(0.856–1.716)	0.278	1.242(0.878–1.756)	0.221
Child–pugh score (B versus A)	1.359(0.924–1.999)	0.120	1.339(0.911–1.969)	0.137
Tumor number (multiple versus single)	2.397(1.726–3.329)	< 0.001	2.391(1.724–3.316)	< 0.001
Maximal tumor size (> 5 versus ≤ 5 cm)	2.511(1.839–3.429)	< 0.001	2.317(1.705–3.151)	< 0.001
Tumor encapsulation (absent versus present)	3.058(2.239–4.177)	< 0.001	2.897(2.127–3.946)	< 0.001
Microvascular invasion (present versus absent)	2.213(1.624–3.016)	< 0.001	2.268(1.668–3.083)	< 0.001
Tumor differentiation (III- IV versus I-II)	3.539(2.561–4.890)	< 0.001	3.444(2.503–4.739)	< 0.001
TNM stage (III versus I-II)	5.481(3.913–7.675)	< 0.001	5.875(4.196–8.225)	< 0.001
ETV1 (positive versus negative)	2.218(1.629–3.020)	< 0.001	2.220(1.635–3.014)	< 0.001
Multivariate analysis				
Tumor number (multiple versus single)	1.272(0.852–1.898)	0.239	1.236(0.823–1.857)	0.307
Maximal tumor size (> 5 versus ≤ 5 cm)	1.146(0.790–1.662)	0.473	1.013(0.704–1.456)	0.946
Tumor encapsulation (absent versus present)	1.495(0.986–2.269)	0.059	1.394(0.923–2.105)	0.114
Microvascular invasion (present versus absent)	1.475(0.995–2.188)	0.053	1.625(1.101–2.399)	0.015
Tumor differentiation (III- IV versus I-II)	1.727(1.195–2.495)	0.004	1.696(1.180–2.437)	0.004
TNM stage (III versus I-II)	2.968(1.885–4.672)	< 0.001	3.518(2.230–5.550)	< 0.001
ETV1 (positive versus negative)	1.636(1.173–2.283)	0.004	1.638(1.180–2.274)	0.003

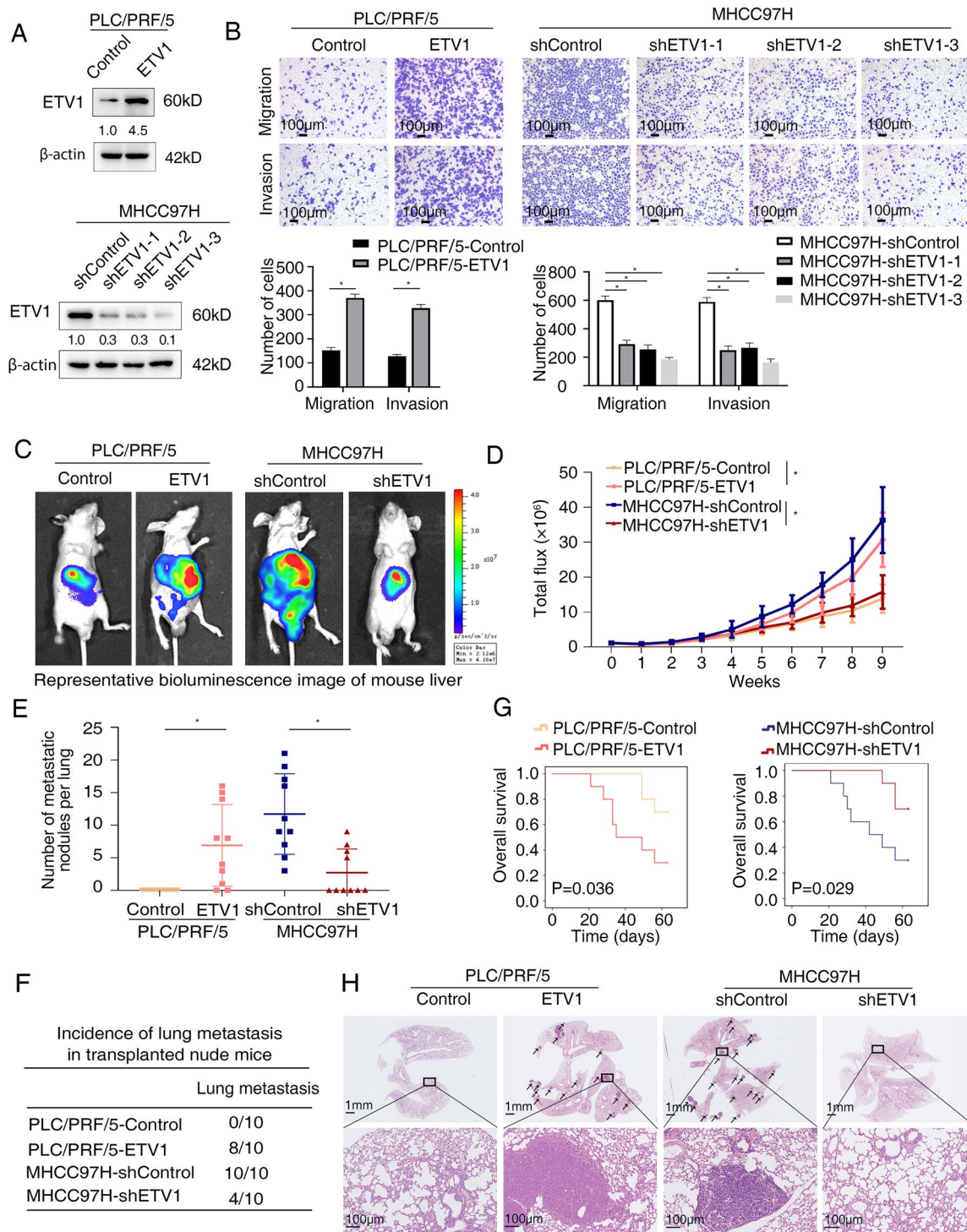


Fig. 2 ETV1 promotes HCC metastasis in vitro and in vivo. **(A)** The efficiency of ETV1-overexpression and ETV1-knockdown in the indicated HCC cells was detected by western blotting. **(B)** Effects of ETV1 overexpression and knockdown on HCC cell migration and invasion. Scale bar, 100 µm. **(C-H)** In vivo metastatic assay. **(C)** The representative BLI images in the liver were shown nine weeks after implanting with indicated cells. **(D)** The bioluminescent signals were used to show the growth rate of liver tumors. **(E)** The number of metastatic lesions in the lung tissues. **(F)** The occurrence of lung metastasis. **(G)** The OS of different groups in the in vivo models. **(H)** Representative images of H&E staining of lung samples (indicated by arrowheads) from each group. Scale bars, 1mm(upper), 100µm (lower). * Represented $p < 0.05$. All data were displayed as Mean \pm SD

lung metastasis incidence, and lung metastatic nodules number, together with shortened OS. Contrastingly, the decreased bioluminescence intensity, lung metastasis incidence, lung metastatic nodules number, and prolonged OS were observed in the MHCC97H-shETV1 group, compared with the MHCC97H-shContorl group (Fig. 2 C-H). In addition, in the subcutaneous xenograft model, we observed that stable overexpression of ETV1 increased the size, weight, and Ki-67 expression of tumors, whereas ETV1 knockdown decreased the growth of tumors and diminished the Ki-67(+) cells compared to the control group (Fig. S1 F-H). Taken together, our findings suggested that increased expression of ETV1 was correlated with poor prognosis in patients with HCC and enhanced HCC metastasis.

Metastasis-related genes *PTK2* and *MET* are downstream targets of ETV1

Considering that ETV1-positive HCC displayed aggressive biological behavior, we next explored the mechanism underlying the role of ETV1 in facilitating HCC metastasis. Liver Cancer RT² Profiler PCR Array was investigated with PLC/PRF/5-ETV1 cells, MHCC97H-shETV1 cells, and control cells. Among 84 liver cancer-related genes, there were 15 upregulated genes in PLC/PRF/5-ETV1 cells compared to control cells and 11 down-regulated genes in MHCC97H-shETV1 cells compared to control cells (Table S1 and S2). A total of 6 genes were overlapped, as shown in Fig. 3A. Among these, *PTK2* and *MET* were the most greatly changed genes and selected for further analysis. TCGA and GEO data indicated that there was a positive correlation between *ETV1* and *PTK2*, *ETV1* and *MET* (Fig. S1 I). Then we conducted RT-qPCR and western blotting to evaluate the impact of ETV1 on two candidates. Congruously, *PTK2* and c-MET were significantly upregulated when ETV1 was overexpressed, and they were both down-regulated following ETV1 knockdown (Fig. 3B, C).

To further elucidate whether ETV1 regulates these two genes, luciferase reporter assays were performed. It indicated that exogenous expression of ETV1 enhanced the activity of *PTK2* and *MET* promoters (Fig. 3D). Several putative ETV1 binding sites were identified in *PTK2* promoter ($n=3$) and *MET* promoter ($n=4$) via bioinformatics analysis (Fig. S2 and S3). Then we generated a series of truncated reporters with deletions in the *PTK2* promoter sequence (Table S3). Luciferase reporter assays showed that deleting the sequence between -575 and -43 base pairs significantly decreased the activity of the *PTK2* promoter enhanced by ETV1 overexpression. Consistent with this, site-directed mutagenesis and luciferase assays indicated that mutation of the putative ETV1-binding site 1 and site 2 located between

-575 to -43 base pairs decreased ETV1-mediated *PTK2* promoter activity (Fig. 3E). The same method was performed for the identification of the specific binding sites of ETV1 in the *MET* promoter. Through serial deletion and site-directed mutagenesis, putative binding site 1 located in the region between -244 and -54 bp was found to mediate ETV1-induced *MET* transactivation (Fig. 3F). Moreover, the direct binding of ETV1 to the promoter region of these two genes described above in HCC cells and specimens was validated by chromatin immunoprecipitation (ChIP) assay (Fig. 3G, H). Together, these data suggested that ETV1 was directly bound to the *PTK2* and *MET* promoters to transcriptionally upregulate their expression.

ETV1 promotes HCC metastasis through upregulating *PTK2* and c-MET expression

PTK2, also known as FAK, is both a non-receptor tyrosine kinase and an adaptor protein with roles in cell migration, motility, invasion, and adhesion signaling [32]. It is overexpressed in multiple cancers and associated with cancer progression and metastasis [33]. In HCC, *PTK2* overexpression is associated with capsular invasion, intrahepatic metastasis, and TNM stage in the detection of human samples [34]. c-MET, encoded by *MET*, plays a central role in promoting tumor invasive growth and driving cancer progression towards metastasis [35]. To address the effects of *PTK2* and c-MET on ETV1-mediated HCC metastasis, we downregulated *PTK2* and c-MET expression in PLC/PRF/5-ETV1 cell line and upregulated *PTK2* and c-MET expression in MHCC97H-shETV1 cell line with lentiviral infection (Fig. S4A, B, Fig. 4A and Table S4). Compared to the controls, *PTK2* or c-MET knockdown decreased the migratory and invasive ability of ETV1-overexpressing HCC cells, whereas *PTK2* or c-MET overexpression increased the migratory and invasive ability reduced by the ETV1 down-regulation (Fig. 4B).

More importantly, the involvement of *PTK2* and c-MET in ETV1-mediated HCC metastasis was further verified in vivo. As shown in Fig. 4 C-H, *PTK2* or c-MET knockdown in PLC/PRF/5-ETV1 orthotopic group reduced bioluminescence intensity, lung metastasis incidence, and lung metastatic nodules number and extended the survival of mice compared with the control group. Reciprocally, the bioluminescence intensity, lung metastasis incidence, and lung metastatic nodules number were increased when *PTK2* or c-MET overexpression compared to the control group. The survival of tumor-bearing mice was shortened via *PTK2* and c-MET overexpression. Together, these findings indicated that *PTK2* and c-MET were crucial to ETV1-mediated HCC metastasis.

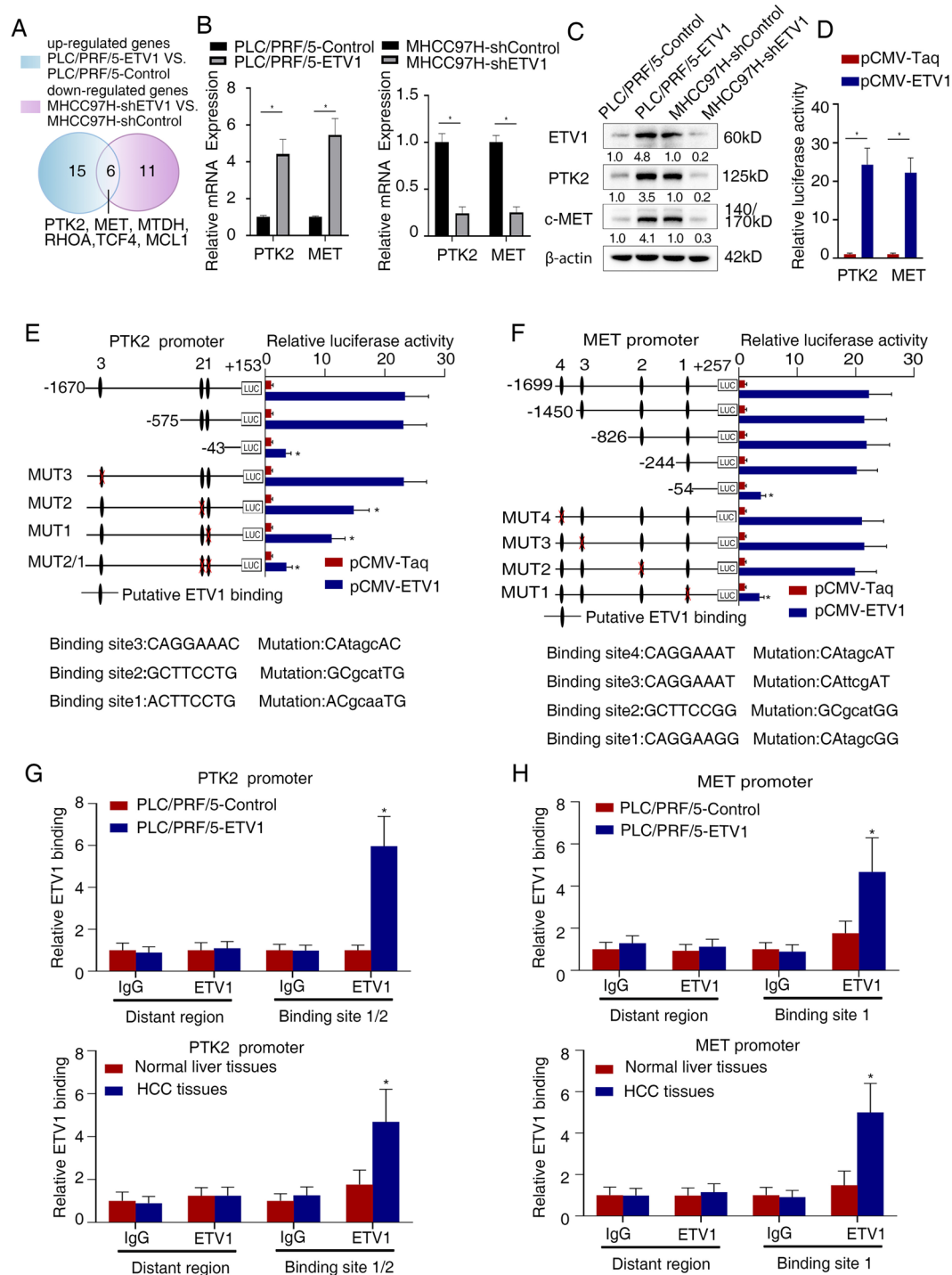


Fig. 3 ETV1 transcriptionally upregulates PTK2 and c-MET expression. **(A)** Human Liver Cancer PCR Array was employed for detecting the upregulated genes in PLC/PRF/5-ETV1 and down-regulated genes in MHCC97H-shETV1 cells compared with controls (fold change ≥ 2.0). Overlapping genes were shown in the Venn diagram. **(B-C)** Compared with the controls, PTK2 and c-MET were upregulated when ETV1 was overexpressed in PLC/PRF/5 cells, and they were down-regulated when ETV1 was knocked down in MHCC97H cells, detected by qRT-PCR and western blotting. **(D)** Relative luciferase activity of PTK2 and MET promoter reporter vectors after cotransfection of pCMV-ETV1 and PTK2 or MET plasmid constructs in PLC/PRF/5 cells. **(E-F)** Relative luciferase activity of indicated PLC/PRF/5 cells cotransfected with pCMV-ETV1 and truncated or mutated luciferase constructs. **(G-H)** ChIP assay of ETV1 binding to the PTK2 or MET promoter in PLC/PRF/5 cells, as well as HCC specimens. * Represented $p < 0.05$. All data were displayed as Mean \pm SD

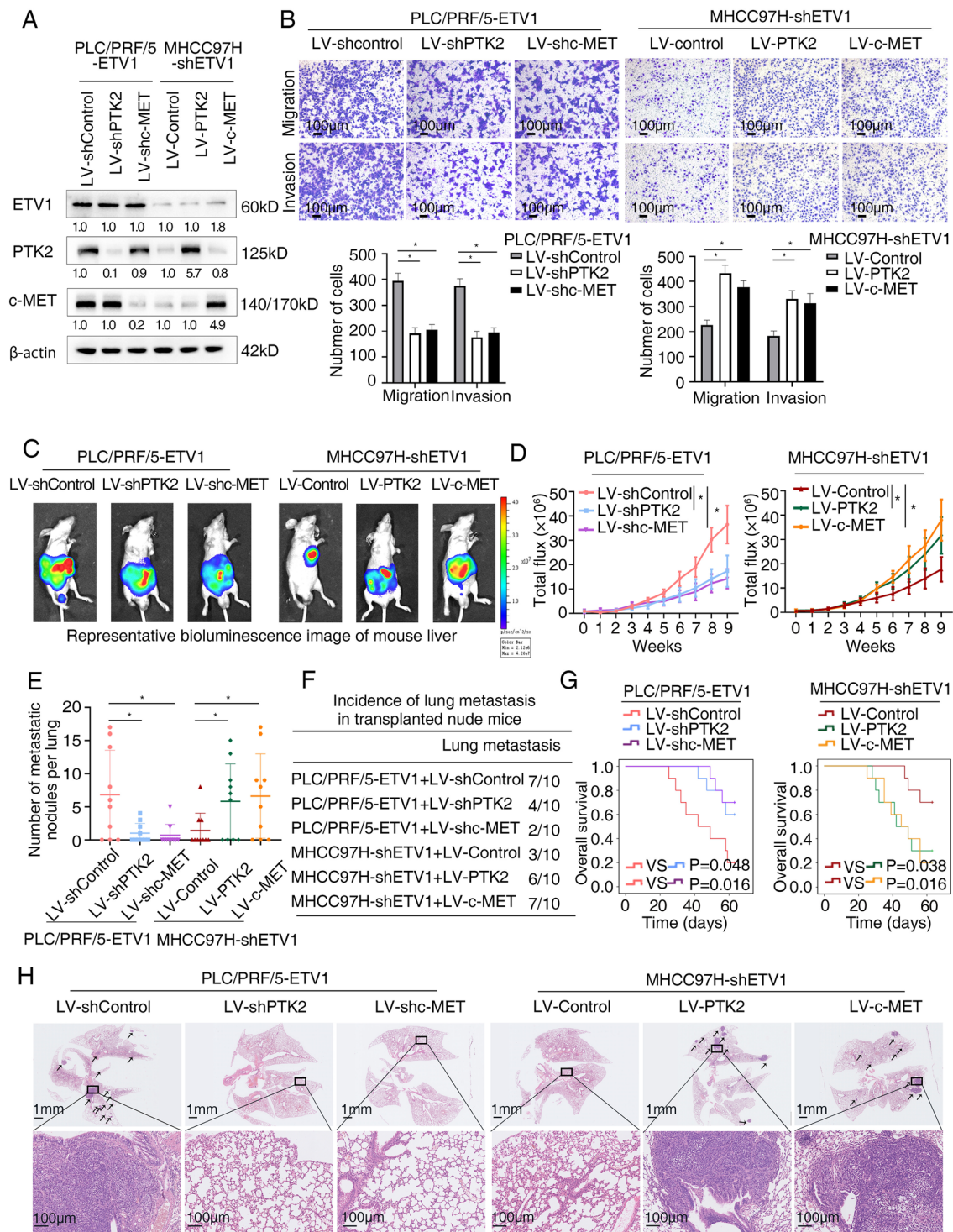


Fig. 4 ETV1 promotes HCC metastasis by upregulating PTK2 and c-MET. **(A)** The levels of ETV1, PTK2, and c-MET in HCC cells after transfected with indicated lentivirus. **(B)** The migratory and invasive capacity were determined by transwell assays in the indicated HCC cells. **(C-H)** In vivo metastatic assay. **(C)** The representative BLI images in the liver were shown 9 weeks after implantation with indicated cells. **(D)** The bioluminescent signals were used to show the growth rate of liver tumors. **(E)** The number of metastatic lesions in the lung tissues. **(F)** The occurrence of lung metastasis. **(G)** The OS of different groups of nude mice. **(H)** Representative images of H&E staining of lung samples (indicated by arrowheads) from each group. * Represented $p < 0.05$. All data were displayed as Mean \pm SD

Besides *PTK2* and *MET*, we detected the expression levels of four other overlapped genes. The mRNA and protein level of *MTDH*, *RHOA*, *TCF4*, *MCL1* were up-regulated when *ETV1* was overexpressed (Figure S5A, B). However, in transwell assays, knockdown of *MTDH*, *RHOA*, *TCF4* and *MCL1* slightly or moderately decreased migration and invasion ability increased by overexpression of *ETV1* in PLC/PRF/5 cells (Figure S5C). These results indicated that *MTDH*, *RHOA*, *TCF4* and *MCL1* were not the main targets for *ETV1*-induced migration and invasion of HCC cells.

HGF/c-MET axis upregulates *ETV1* via ERK1/2 activation

Given that *ETV1* was significantly upregulated in HCC and promoted the malignant progression of HCC, we sought to investigate the molecular mechanisms facilitating *ETV1* upregulation in HCC. Since c-MET contributed to the aggressive peculiarities of *ETV1*-overexpressing HCC, its well-known ligand HGF attracted our attention. Binding to c-MET, HGF acts as a trigger for various cellular processes. In cooperation with GDNF, HGF induces *ETV4* expression in spinal cord explants for recruitment of motor neurons, meanwhile, *ETV4* is also required for the induction of c-Met expression by GDNF [36]. c-Met signaling regulates the expression the PEA3 factors to promote cell migration and invasion in gastric and lung cancer cells with MET-addicted [37]. HGF upregulates *ETV5* to promote cell invasion of oral squamous cell carcinoma [38]. These studies suggested that the HGF/c-Met axis might be involved in regulation of PEA3 subfamily. We were interested in whether HGF is a regulator of *ETV1* in HCC.

We treated PLC/PRF/5 cells with different concentrations of recombinant HGF. HGF increased the *ETV1* mRNA and protein expression levels in a dose-dependent manner. Similar results were observed in HepG2 cells with relatively low *ETV1* expression (Fig. 5A, B). Luciferase reporter assay demonstrated that *ETV1* promoter activity was augmented upon HGF treatment (Fig. 5C). HGF/c-MET axis activates several signaling cascades, including MAPK and PI3K/Akt. PI3K inhibitor LY294002, ERK1/2 inhibitor SCH772984, JNK inhibitor SP600125, and p38 inhibitor SB203580 were applied to treat PLC/PRF/5 cells. SCH772984 significantly diminished HGF-induced *ETV1* expression, while other inhibitors did not have such effect (Fig. 5D). ERK1/2 was also knockdown with shRNA to determine its effect on *ETV1* expression upon HGF treatment. As shown in Fig. S6A, knockdown of ERK1/2 decreased the *ETV1* level upregulated upon HGF treatment. These data suggested that HGF upregulated *ETV1* via ERK1/2 pathway.

To specify important *cis*-regulatory elements in the *ETV1* promoter, we analyzed the *ETV1* promoter and searched for putative transcription factor binding sites (Fig. 5E). We constructed a series of truncations/mutations of the *ETV1* promoter sequence (Fig. S7 and Fig. 5E). Promoter activity of the constructs induced by HGF was decreased between -463 bp to -70 bp, suggesting this region was vital to regulate the activity of *ETV1* promoter (Fig. 5E). Mutant constructs for the ELK1, ETS1, and SP-1 binding sites were generated using point mutagenesis. Of these mutant constructs, mutants of one ELK1 binding site, binding site 1, in this region showed a significant reduction in activity (Fig. 5E). Knockdown of ELK1 abolished the increased activity of *ETV1* promoter and the upregulated *ETV1* expression level induced by HGF (Fig. 5F-H and Fig. S4C). Further, the ChIP assay validated that SCH772984 mitigated the binding of ELK1 to the *ETV1* promoter in PLC/PRF/5 cells treated by HGF, whereas other inhibitors had no such obvious effect (Fig. 5I). Moreover, we detected the serum HGF levels in the HCC patients by ELISA and detected the *ETV1* levels in the tumor tissues of HCC patients by IHC (Fig. S8A). The correlation analysis showed that *ETV1* score (0–12) positively correlated with the levels of serum HGF ($r=0.4970$, $P=0.005$) in the HCC patients ($n=30$) (Fig. S8B). And positive correlations between *ETV1* and *HGF*, *ETV1* and *ELK1* expression were observed in TCGA and GEO databases (Fig. S8C, D). Accordingly, the ERK1/2-ELK1 cascade was responsible for an augmented level of *ETV1* induced by HGF. HGF upregulated *ETV1* expression via c-MET-ERK1/2-ELK1 cascade, which in turn upregulated c-MET expression, forming a positive feedback.

ETV1 is vital for HGF-mediated HCC invasion and metastasis

In HCC, HGF is expressed by stromal cells or tumor cells and binds to its specific receptor, c-MET, to play a part in tumor onset, proliferation, invasion and metastasis [39]. The serum level of HGF is associated with extrahepatic metastasis [40, 41]. HGF induced by hepatectomy could promote metastasis of residual HCC cells [42]. Mechanistically, HGF regulates HCC invasion and metastasis by promoting EMT, activating signaling pathways, upregulating MMPs and so on [39]. Given the significance of HGF in HCC invasion and metastasis, we processed to test whether *ETV1* contributes to HGF-induced HCC metastasis. Recombinant HGF was used to treat *ETV1*-knockdown PLC/PRF/5 cells (Fig. 6A). The promoting effects on cell migration and invasion enhanced by HGF were dampened when *ETV1* was knockdown (Fig. 6B). Then we generated stable PLC/PRF/5-HGF cell line and knockdown *ETV1* expression with shRNA. Exogenous

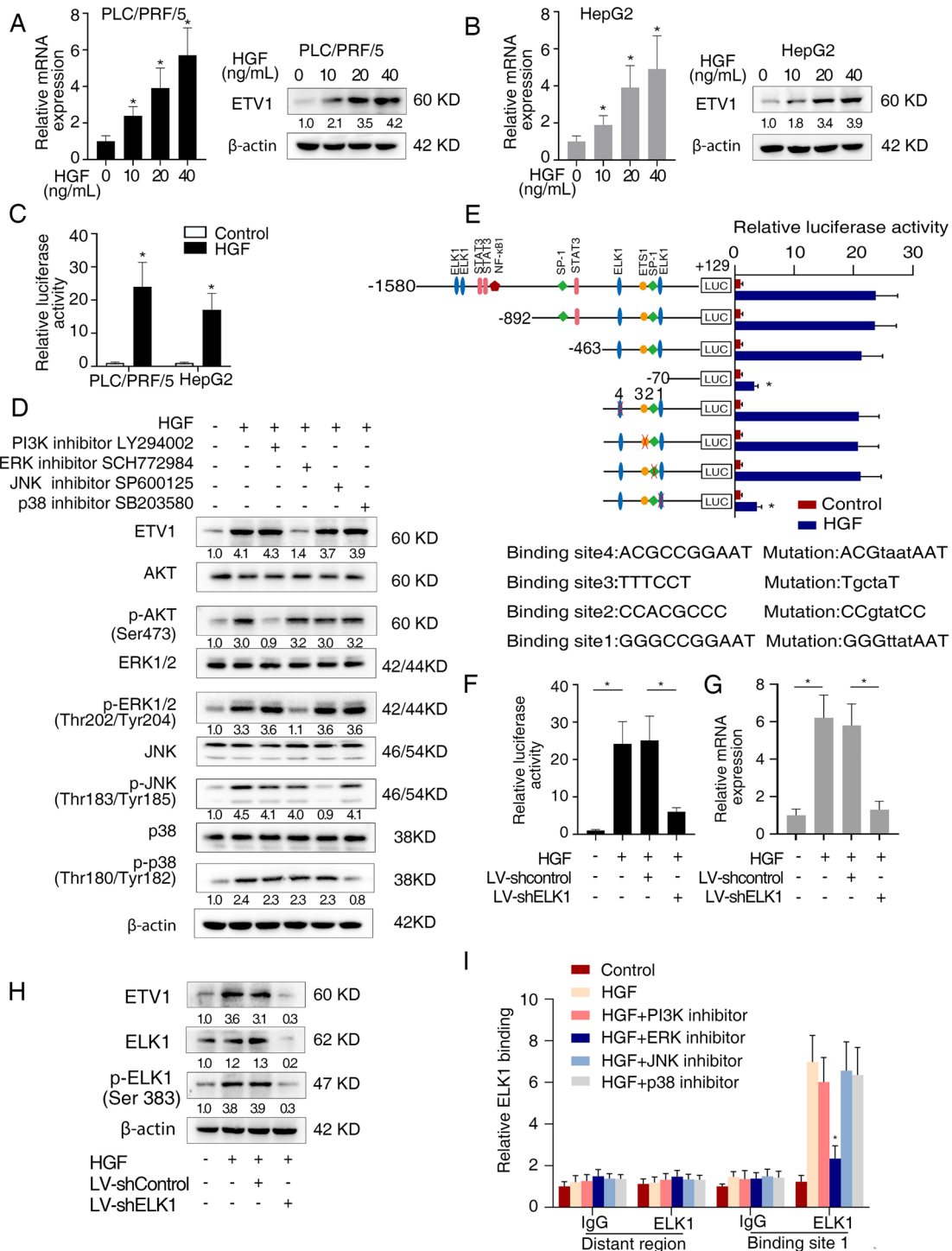


Fig. 5 HGF/c-MET axis upregulates ETV1 via ERK1/2 activation. **(A)** The expression of ETV1 in PLC/PRF/5 cells treated with different concentrations of recombinant HGF. **(B)** The expression of ETV1 in HepG2 cells treated with different concentrations of HGF. **(C)** Relative luciferase activities of ETV1 promoter reporter vectors in indicated cells upon treatment with HGF. **(D)** Western blotting assays of ETV1, Akt, p-Akt, ERK1/2, p-ERK1/2, JNK, p-JNK, p38, p-p38, proceed with PI3K inhibitor (LY294002), ERK1/2 inhibitor (SCH772984), JNK inhibitor (SP600125), and p38 inhibitor (SB203580) upon HGF treatment in PLC/PRF/5 cells. **(E)** Relative luciferase reporter assays of PLC/PRF/5 cells transfected with serially truncated or mutant ETV1 promoter luciferase constructs treated with or without HGF. **(F-H)** The relative promoter luciferase activity, mRNA, and protein levels of ETV1 in the PLC/PRF/5 cells after transfection with shELK1 or control shRNA in the presence of HGF. **(I)** ChIP assays verified the direct binding of ELK1 to the ETV1 promoter in HCC cells. * Represented $p < 0.05$. All data were displayed as Mean \pm SD

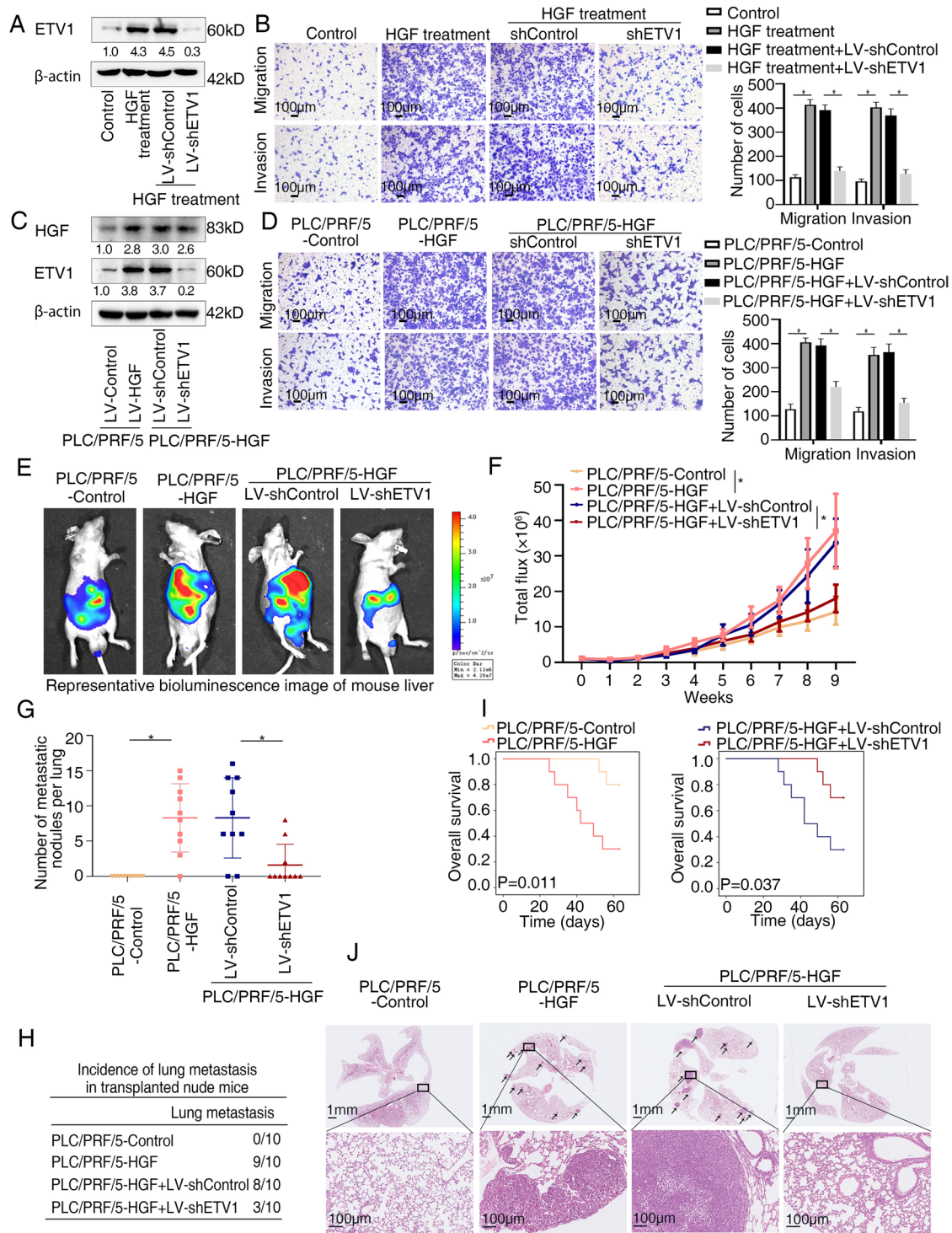


Fig. 6 ETV1 is vital for HGF-mediated HCC invasion and metastasis. **(A)** The protein levels of ETV1 in the PLC/PRF/5 cells transfected with LV-shControl or LV-shETV1 upon HGF treatment. **(B)** Transwell assays displayed the migratory and invasive capacity of the indicated cells upon HGF treatment. **(C)** The levels of HGF and ETV1 in the PLC/PRF/5-HGF cells transfected with LV-shControl or LV-shETV1. **(D)** Transwell assays displayed the migratory and invasive capacity of the indicated cells. **(E-J)** In vivo metastatic assay. **(E)** The representative BLI images in the liver were shown 9 weeks after implantation with indicated cells. **(F)** The bioluminescent signals were used to show the growth rate of liver tumors. **(G)** The number of metastatic lesions in the lung tissues. **(H)** The occurrence of lung metastasis. **(I)** The OS of different groups of nude mice. **(J)** Representative images of H&E staining of lung samples (indicated by arrowheads) from each group. * Represented $p < 0.05$. All data were displayed as Mean \pm SD

HGF expression and knockdown of endogenous ETV1 in the indicated cells were confirmed by western blotting (Fig. 6C). Transwell assays demonstrated that downregulation of ETV1 inhibited the promoting effects of HGF-overexpressing on cell invasion and migration (Fig. 6D). Since ERK1/2 inhibitor inhibited ETV1 upregulation induced by HGF (Fig. 5D), to better ascertain the role of ERK1/2-ETV1 in HGF-mediated HCC cell invasion and migration, we investigated the effect of ERK1/2 inhibitor SCH772984 on migration and invasion of PLC/PRF/5 cells mediated by recombinant HGF. The results exhibited that promoting effects on cell migration and invasion enhanced by HGF were dampened when treated with ERK1/2 inhibitor (Fig. S9A). Similarly, SCH772984 treatment inhibited the increase of cell migration and invasion induced by HGF overexpression (Fig. S9B).

Consistent with our data in vitro, the results of in vivo models exhibited that compared with the control group, the HGF-overexpressing group demonstrated dramatically increased bioluminescence intensity, lung metastasis incidence, and lung metastatic nodules number, as well as shortened overall survival. Contrastingly, these HGF-induced phenotypes were decreased when ETV1 was knocked down (Fig. 6E-J). Data above suggested that ETV1 was important for HGF-mediated HCC metastasis.

ETV1 expression correlates with PTK2 and c-MET expression in HCC specimens

On account of the contribution of ETV1 to HCC metastasis, we next performed IHC assays and correlation analysis to explore whether there is a clinical relevance of ETV1 with its two downstream targets. In two HCC patient cohorts (cohort I, $n=260$; cohort II, $n=280$), ETV1 expression was correlated with PTK2 and c-MET expression (Fig. 7A, B), and elevated expression of PTK2 or c-MET was associated with poor tumor differentiation, microvascular invasion, loss of encapsulation, and advanced TNM stage (Table S5 and S6). Moreover, patients with positive PTK2 or c-MET expression had higher recurrence rates and shorter OS than patients with negative PTK2 or c-MET expression (Fig. 7C). Subpopulations with ETV1/PTK2 or ETV1/c-MET coexpression had the highest recurrence rates and the shortest OS, as illustrated by Kaplan–Meier curves (Fig. 7D).

In addition, the mRNA and protein levels of ETV1, PTK2, and c-MET were detected in 20 cases of paired primary and metastatic specimens, and they were the highest in metastatic ones compared with primary HCC and adjacent nontumorous specimens (Fig. S10A-C).

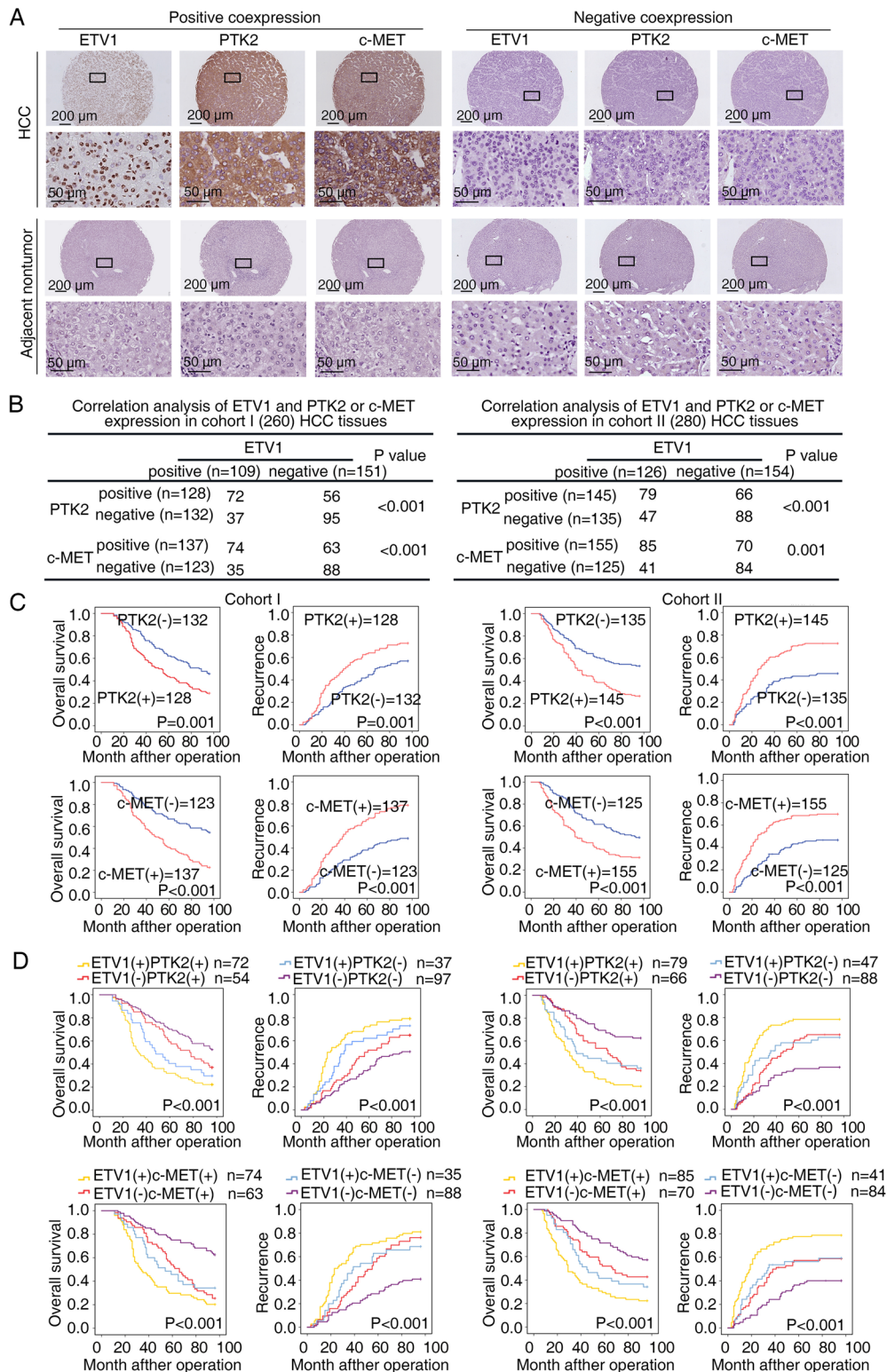
The combination of defactinib with capmatinib is effective in reducing ETV1-mediated HCC metastasis

Defactinib is a leading PTK2 inhibitor investigated in several clinical trials in combination with other agents.

It functions via inhibition of phosphorylation of Tyr-397, a critical target of PTK2 activation [32, 43]. Capmatinib is a highly selective tyrosine kinase inhibitor targeting c-MET. It was approved by the FDA for patients with metastatic non-small cell lung cancer harboring *MET* exon 14 skipings based on the GEOMETRY mono-1 study in 2020 [44]. Given the significance of PTK2 and c-MET in ETV1-mediated HCC metastasis, we next evaluated the antitumor efficacy of the two inhibitors mentioned above. The efficacy of defactinib plus capmatinib was verified by decreased expression of p-PTK2 (Tyr397) and p-c-MET (Tyr1234/1235) (Fig. 8A). Intriguingly, transwell assays exhibited that the combination treatment of defactinib and capmatinib significantly decreased migratory and invasive ability of PLC/PRF5-ETV1 cells, whereas treatment with defactinib or capmatinib alone played a partial inhibitory effect (Fig. 8B). Similar results were observed in the in vivo models. Compared to the control group, treatment with defactinib or capmatinib alone partially reduced lung metastasis incidence together with lung metastatic nodules number and improved the OS to some extent, whereas the combined treatment significantly decreased bioluminescence intensity, lung metastasis incidence, lung metastatic nodules number, and prolonged the survival of the nude mice (Fig. 8C-I). Altogether, these findings demonstrated that the combination therapy with PTK2 inhibitor defactinib and c-MET inhibitor capmatinib inhibited HCC metastasis induced by ETV1 expression.

Discussion

Metastasis is the main factor of poor prognosis in patients with HCC [2]. It is of great significance to gain insight into its mechanisms. As a member of ETS/PEA3 family, ETV1 has been well documented to represent oncogenic drivers across several tumors including prostate cancer, Ewing sarcoma and GIST [21, 45, 46]. Besides, authors have reported its clinical significance. High ETV1 levels are correlated with shorter prostate-specific antigen (PSA) recurrence in prostate cancer, while nuclear overexpression of ETV1 is associated with longer overall survival in esophageal adenocarcinoma [47, 48]. Functionally, ETV1 influences tumor progression by inducing EMT, promoting cell migration and invasion, regulating cell cycle and apoptosis, as well as mediating chemotherapy resistance [12]. However, its expression and role in HCC remain elusive. In this study, we found the elevated expression of ETV1 in HCC specimens and a close correlation between high ETV1 expression and advanced TNM stage, microvascular invasion, and loss of encapsulation. More crucially, multivariable Cox regression implied that elevated expression of ETV1 was a valuable indicator for poor prognosis in HCC.



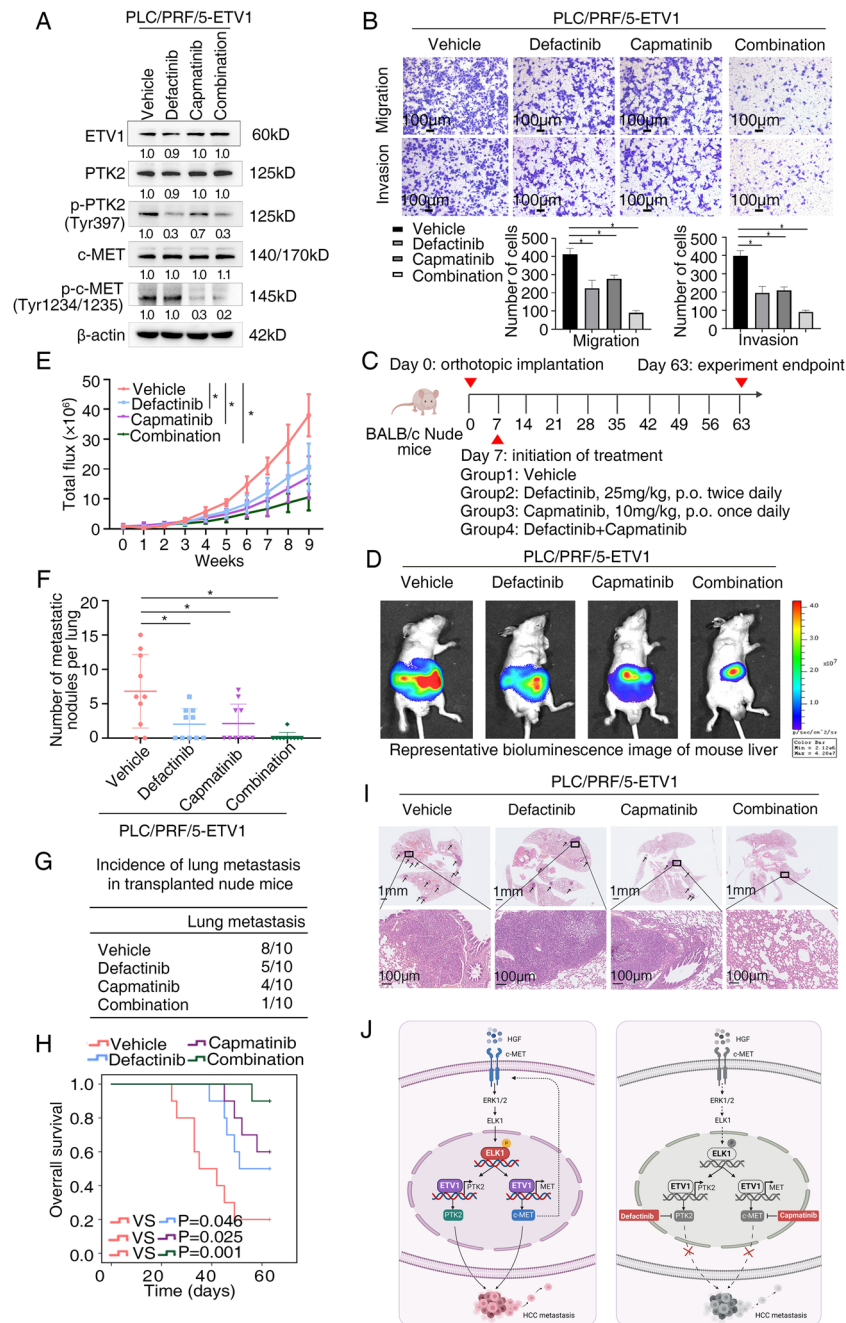


Fig. 8 The combination of defactinib with capmatinib is effective in reducing ETV1-mediated HCC metastasis **(A)** The levels of ETV1, p-PTK2 (Tyr397), PTK2, p-c-MET (Tyr1234/1235), c-MET in PLC/PRF/5-ETV1 cells processed with a single agent or the combination of defactinib and capmatinib. **(B)** HCC cell invasion and migration was evaluated by transwell assay. The combination treatment of defactinib and capmatinib showed the greatest inhibitory effect among all the groups. **(C)** Schematic diagram of treatment in nude mice of four groups. (Group1: Vehicle, Group2: Defactinib, Group3: Capmatinib, Group4: Defactinib combined with Capmatinib) **(D-I)** In vivo metastatic assay. **(D)** The representative BLI images in the liver were shown 9 weeks after implantation with indicated cells. **(E)** The bioluminescent signals were used to show the growth rate of liver tumors. **(F)** The number of metastatic lesions in the lung tissues. **(G)** The occurrence of lung metastasis. **(H)** The OS of different groups of nude mice. **(I)** Representative images of H&E staining of lung samples (indicated by arrowheads) from each group. * Represented $p < 0.05$. All data were displayed as Mean \pm SD. **(J)** Diagram illustrating the mechanisms underlying how ETV1 promotes HCC metastasis and a potential combination strategy. ETV1 mediates HCC metastasis through increasing PTK2 and c-MET expression. HGF upregulates ETV1 expression via c-MET-ERK1/2-ELK1, creating a positive feedback loop that continuously stimulates HCC development. PTK2 inhibition in combination with c-MET inhibition markedly mitigates ETV1-mediated HCC metastasis

Compared with normal specimens, metastatic specimens had higher ETV1 levels than primary specimens. By transwell assays and the orthotopically metastatic model, we proved that ETV1 was critical for invasion and metastasis of HCC. Altogether, both clinical findings and functional studies suggested that ETV1, a transcription factor, whose expression was associated with prognosis of HCC patients, displayed a potent promoting effect on HCC metastasis.

ETV1 binds to many target genes and plays a role in tumor progression and metastasis by regulating expression of them. It has previously been shown to confer the aggressive biologic behavior of tumors via inhibition of checkpoint kinase 1 (*CHK1*), upregulation of EMT-associated genes such as *TWIST1*, *SNAIL*, *HAS2*, pro-metastatic genes such as *MMP1/7*, *SPARC*, methyltransferase *METTL3* [20, 49–53]. Herein, we uncovered that PTK2 and c-MET were transcriptional targets of ETV1. PTK2 is an important signaling “hub”, primarily regulating adhesion signaling and cell migration, as well as cell survival under stress [32]. In HCC, PTK2 expression is frequently increased and is responsible for HCC cell invasion and migration, partially through regulating MMP2 and MMP9 [54, 55]. In particular, studies reported that elevated PTK2 and p-PTK2 Tyr397 levels are correlated with vascular invasion and intrahepatic metastasis, offering a promising target to treat HCC [54, 56]. c-MET is known to exert oncogenic functions in HCC [22]. It is reported that MET-regulated gene expression signature has a close correlation with increased vascular invasion and microvessel density in HCC patients [57]. c-MET regulates cell migration and invasion through activating its downstream effector including RAS/MAPK, PI3K/Akt and RAC1/CDC42 pathways. It can also promote HCC metastasis through regulating mitochondrial fission [58]. Accordingly, both PTK2 and c-MET play significant roles in HCC invasion and metastasis. Herein, PTK2 and c-MET were identified as transcriptional targets of ETV1. PTK2 or c-MET knockdown impeded ETV1-mediated HCC metastasis. Reciprocally, PTK2 or c-MET overexpression rescued HCC metastasis inhibited by ETV1 knockdown. In two HCC patient cohorts, ETV1 expression was positively associated with PTK2 and c-MET expression. It was noted that coexpression of ETV1/PTK2 or ETV1/c-MET subpopulations displayed the poorest OS and the highest recurrence rate. These results verified that PTK2 and c-MET were required for the promoting effect of ETV1 on HCC metastasis.

The regulatory mechanism of ETV1 overexpression in human HCC remains unknown. Prior studies have reported that ETV1 expression can be regulated by several ways. FOXF1 transcriptionally regulates ETV1 mainly through enhancer binding. FOXF1 co-localizes

with ETV1 at enhancers to regulate the ETV1-dependent GIST-lineage specific transcriptome [59]. Constitutive photomorphogenetic 1 (COPI) and capicua (CIC) have been identified as repressors of ETV1. COPI regulates the expression of ETV1 at post-translational level by directly binding to its N-terminus and leading to the ubiquitination degradation [60]. CIC is a transcriptional repressor of the HMG-box family which binds specific DNA sites in target genes [61]. The well-characterized mammalian targets of CIC are ETV1/4/5. Dysregulation of CIC induced de-repression of ETV1/4/5 was found to negatively affect patient prognosis or drive aggressive phenotypes [62]. Moreover, ETV1 is reported to be significantly upregulated by FGF2 treatment and downregulated by TGF- β 1, thus generating distinct cancer-associated fibroblasts populations to promote skin squamous cell carcinoma development [63]. In HCC, we observed that HGF upregulated ETV1 in a dose-dependent way. Previous study reported that the ERK1/2 and p38 inhibitors affect the ETV1 level in colorectal cancer cells [64]. Our results showed that inhibition of the ERK1/2 pathway diminished HGF-induced ETV1 expression, whereas other inhibitors had no such effect. The overexpression of ETV1 upregulated the expression of c-MET, which in turn enhanced HCC sensitivity to HGF stimulation, thus creating a positive feedback loop. HGF-c-MET axis plays a part in augmenting HCC angiogenesis, invasion, and metastasis [41]. Consistent with this, our data suggested that migration and invasion of HCC cells were enhanced under HGF treatment, whereas ETV1 knockdown decreased the migration and invasion capability of HCC cells enhanced by HGF.

To find an effective way of inhibiting HCC metastasis mediated by ETV1, we focused on pharmacological inhibitors of PTK2 and c-MET. Due to the significance of PTK2, PTK2 inhibitors are being actively developed, showing well tolerability [65]. Defactinib (VS-6063), an ATP-competitive PTK2 inhibitor, functions via inhibiting phosphorylation of Tyr397 and downstream pathways [66]. Defactinib can impede the initiation of liver cancer and ameliorate the efficacy of sorafenib in HCC [67]. Nonetheless, one phase II study showed that defactinib has only modest antitumor activity [68]. In our study, treatment with defactinib alone partially reduced migration and invasion capability of PLC/PRF/5-ETV1 HCC cells and slowed down HCC growth. We observed the similar effect of c-MET inhibitor on HCC metastasis. Given the role of PTK2 and c-MET in ETV1-mediated metastasis and the discovery of the HGF-ETV1-c-MET loop, we speculated that c-MET inhibitors might cooperate with PTK2 inhibitors in targeting ETV1-overexpressing HCC. c-Met inhibitors have shown antitumor potential in preclinical models,

and many of them are currently in clinical trials for cancer [69]. Regrettably, the benefits of these drugs applied alone have not been as impressive as initially hoped [5]. Capmatinib is a highly potent MET inhibitor with manageable safety, found to be highly selective for c-MET over other kinases. Tumor regression was observed on a liver cancer xenograft model treated with capmatinib [70]. Our data illustrated that the combination of defactinib plus capmatinib conspicuously promoted anti-HCC efficacy in vitro and in vivo, and the combined treatment may have utility for HCC patients with ETV1 overexpression. However, this aspect warrants further investigation.

In conclusion, we demonstrated that ETV1 was frequently increased in HCC, mainly promoted by HGF. HGF/c-MET axis enhanced ETV1 expression via ERK1/2-ELK1 pathway, leading to PTK2 and c-MET upregulation and subsequent augmented HCC metastasis. Targeting the HGF-ETV1-PTK2/c-MET axis may provide evidence for developing a novel treatment strategy to ameliorate HCC progression.

Conclusions

Our study shows that increased ETV1 expression functionally contributes to HCC metastasis. In addition, ETV1 abundance correlates with patient survival and recurrence and thus may have prognostic value for patients with HCC. Mechanistically, ETV1 upregulates PTK2 and c-MET expression, and HGF upregulates ETV1 expression through c-MET-ERK1/2-ELK1 pathway, forming a positive feedback loop. Combined treatment of defactinib and capmatinib significantly suppressed HCC metastasis, which may provide a potential targeting strategy for HCC treatment.

Abbreviations

ETS: E-twenty-six transformation-specific; BLI: Bioluminescence imaging; ChIP: Chromatin immunoprecipitation; c-MET: Tyrosine protein kinase Met; HCC: Hepatocellular carcinoma; H&E: Hematoxylin and eosin; HGF: Hepatocyte growth factor; IHC: Immunohistochemical; MAPK: Mitogen-activated protein kinase; OS: Overall survival; PTK2: Protein tyrosine kinase 2; RT-qPCR: Quantitative reverse transcription-polymerase chain reaction; shRNA: Short hairpin RNA; TNM: Tumor-nodule-metastasis.

Supplementary Information

The online version contains supplementary material available at <https://doi.org/10.1186/s13046-022-02475-2>.

Additional file 1: Supplementary materials. Figure S1. (A) ETV1 expression in LIHC and correlation of ETV1 expression with overall survival were analyzed in LIHC according to the data of The Cancer Genome Atlas (TCGA). (B) Cell Counting Kit-8 (CCK8) assay assessing the cell proliferation of the ETV1-overexpressing PLC/PRF/5 cells and ETV1-knockdown MHCC97H cells. (C) Colony formation assay showing the proliferation of the indicated HCC cells. Therepresentative photos were shown and the cell numbers were quantified. (D-F) Tumorgrowth of the indicated

HCC cells was assessed by subcutaneous xenograft tumor models. The tumor volume and weight were shown in (D) and (E), the representative images of Ki67 were shown in (F). $n = 5$ in each group. (G) The correlation between ETV1 expression and PTK2 or MET expression in TCGA-LIHC and GEO database. $*p < 0.05$, $****p < 0.0001$. Data were shown as Mean \pm SD. **Figure S2.** ETV1 binding sites within the promoter regions of PTK2. Thesequences highlighted in yellow represent the three binding sites of ETV1 on the PTK2 promoter, and the arrow represents the transcription initiation sites. The mutagenesis of the promoter sequence were annotated. **Figure S3.** ETV1 binding sites within the promoter regions of MET. The sequences highlighted in yellow represent the four binding sites of ETV1 on the MET promoter, and the arrow represents the transcription initiation sites. The mutagenesis of the promoter sequence were annotated. **Figure S4.** (A-C) Western blot verifying PTK2 and MET knockdown effect in PLC/PRF/5-ETV1 cells and ELK1 knockdown effect in PLC/PRF/5 cells. **Figure S5.** (A) The expression levels of MTDH, RHOA, TCF4 and MCL1 were determined in the indicated cells by real-time PCR. (B) Western blotting assays of MTDH, RHOA, TCF4 and MCL1 in the indicated cells transfected with lentivirus. (C) The migrating and invasive capability of the indicated cells was determined via transwell assay. **Figure S6.** (A) The level of ETV1 in the PLC/PRF/5 cells upon HGF treatment with/without ERK1/2 knockdown. **Figure S7.** Transcription factors binding sites within the promoter regions of ETV1. The sequences highlighted in blue represent the four binding sites of ELK1 on the ETV1 promoter. The yellow highlighted sequences represent the one binding site of ETS1 on the ETV1 promoter. The sequences highlighted in grey represent the binding site of SP1 on the ETV1 promoter. The red highlighted sequences represent the binding site of NF- κ B1 on the ETV1 promoter. The pink highlighted sequences represent the binding site of STAT3 on the ETV1 promoter. The arrows represent transcription start sites. The mutagenesis of the promoter sequence were annotated. **Figure S8.** (A) Representative IHC staining of ETV1 is shown. (B) Pearson correlation analyses between ETV1 IHC score and the levels of serum HGF in HCC patients. $n = 30$. (C) The correlation between ETV1 expression and HGF expression in TCGA-LIHC and GEO database. (D) The correlation between ETV1 expression and ELK1 expression in TCGA-LIHC and GEO database. **Figure S9.** Effect of ERK1/2 inhibitor on HGF-mediated HCC cell migration and invasion. (A) Transwell assays displayed the migratory and invasive capacity of the indicated cells upon HGF treatment. (B) Transwell assays displayed the migratory and invasive capacity of the indicated cells. **Supplementary Table S1.** List of genes differentially expressed in PLC/PRF/5-ETV1 versus PLC/PRF/5-Control cells using a human liver cancer PCR array. **Supplementary Table S2.** List of genes differentially expressed in MHCC97H-shETV1 versus MHCC97H-shControl cells using a human liver cancer PCR array. **Supplementary Table S3.** Primer sequences used in the study. **Supplementary Table S4.** Knockdown shRNA sequences used in this study. **Supplementary Table S5.** Correlation between PTK2 expression and clinicopathological characteristics of HCCs in two independent cohorts of human HCC tissues. **Supplementary Table S6.** Correlation between c-MET expression and clinicopathological characteristics of HCCs in two independent cohorts of human HCC tissues.

Acknowledgements

Not applicable.

Authors' contributions

TZ, YW and MX performed the experiments. XJ and XL assisted in immunohistochemistry staining and animal experiments. XC and BZ gave assistance in collecting and providing metastatic HCC samples and gave advice on experimental design. LD, YF, and MS gave assistance in collecting tissues samples and analyzing data. The author(s) read and approved the final manuscript.

Funding

Research was supported by grants from the National Natural Science Foundation of China No. 81972237 (L.X.), No. 82173313 (W.H.), and No. 81871911 (W.H.).

Availability of data and materials

The data supporting our conclusion were obtained from the TCGA database and GEO database.

Declarations

Ethics approval and consent to participate

This study was approved by the Ethics Committee of Tongji Hospital of Tongji Medical College, Huazhong University of Science and Technology. All animal experiments were conducted in accordance with the principles and procedures approved by the Ethics Committee of Tongji Hospital of Tongji Medical College, Huazhong University of Science and Technology.

Consent for publication

All authors have agreed to publish this manuscript.

Competing interests

The authors declare no conflict of interests.

Author details

¹Department of Gastroenterology, Institute of Liver and Gastrointestinal Diseases, Hubei Key Laboratory of Hepato-Pancreato-Biliary Diseases, Tongji Hospital of Tongji Medical College, Huazhong University of Science and Technology, Wuhan 430030, Hubei Province, China. ²Hepatic Surgery Center, Hubei Key Laboratory of Hepato-Pancreato-Biliary Diseases, Tongji Hospital of Tongji Medical College, Huazhong University of Science and Technology, Wuhan 430030, Hubei Province, China. ³Key Laboratory of Organ Transplantation, Ministry of Education and Ministry of Public Health, Wuhan 430030, Hubei, China.

Received: 15 April 2022 Accepted: 24 August 2022

Published online: 16 September 2022

References

- Forner A, Reig M, Bruix J. Hepatocellular carcinoma. *Lancet*. 2018;391(10127):1301–14.
- Ryu SH, Jang MK, Kim WJ, Lee D, Chung YH. Metastatic tumor antigen in hepatocellular carcinoma: golden roads toward personalized medicine. *Cancer Metastasis Rev*. 2014;33(4):965–80.
- Lambert AW, Pattabiraman DR, Weinberg RA. Emerging Biological Principles of Metastasis. *Cell*. 2017;168(4):670–91.
- Gadaleta RM, Moschetta A. Dark and bright side of targeting fibroblast growth factor receptor 4 in the liver. *J Hepatol*. 2021;75(6):1440–51.
- Rimassa L, Assenat E, Peck-Radosavljevic M, Pracht M, Zagonel V, Mathurin P, et al. Tivantinib for second-line treatment of MET-high, advanced hepatocellular carcinoma (METIV-HCC): a final analysis of a phase 3, randomised, placebo-controlled study. *Lancet Oncol*. 2018;19(5):682–93.
- Huang A, Yang XR, Chung WY, Dennison AR, Zhou J. Targeted therapy for hepatocellular carcinoma. *Signal Transduct Target Ther*. 2020;5(1):146.
- Llovet JM, Montal R, Sia D, Finn RS. Molecular therapies and precision medicine for hepatocellular carcinoma. *Nat Rev Clin Oncol*. 2018;15(10):599–616.
- Bruix J, Chan SL, Galle PR, Rimassa L, Sangro B. Systemic treatment of hepatocellular carcinoma: An EASL position paper. *J Hepatol*. 2021;75(4):960–74.
- Finn RS, Qin S, Ikeda M, Galle PR, Ducreux M, Kim TY, et al. Atezolizumab plus Bevacizumab in Unresectable Hepatocellular Carcinoma. *N Engl J Med*. 2020;382(20):1894–905.
- Gordan JD, Kennedy EB, Abou-Alfa GK, Beg MS, Brower ST, Gade TP, et al. Systemic Therapy for Advanced Hepatocellular Carcinoma: ASCO Guideline. *J Clin Oncol*. 2020;38(36):4317–45.
- Sizemore GM, Pitarresi JR, Balakrishnan S, Ostrowski MC. The ETS family of oncogenic transcription factors in solid tumours. *Nat Rev Cancer*. 2017;17(6):337–51.
- Qi T, Qu Q, Li G, Wang J, Zhu H, Yang Z, et al. Function and regulation of the PEA3 subfamily of ETS transcription factors in cancer. *Am J Cancer Res*. 2020;10(10):3083–105.
- Chotteau-Lelievre A, Montesano R, Soriano J, Soulie P, Desbiens X, de Launoit Y. PEA3 transcription factors are expressed in tissues undergoing branching morphogenesis and promote formation of duct-like structures by mammary epithelial cells in vitro. *Dev Biol*. 2003;259(2):241–57.
- Shekhar A, Lin X, Liu FY, Zhang J, Mo H, Bastarache L, et al. Transcription factor ETV1 is essential for rapid conduction in the heart. *J Clin Invest*. 2016;126(12):4444–59.
- Arber S, Ladle DR, Lin JH, Frank E, Jessell TM. ETS gene Er81 controls the formation of functional connections between group Ia sensory afferents and motor neurons. *Cell*. 2000;101(5):485–98.
- Siembab VC, Gomez-Perez L, Rotterman TM, Shneider NA, Alvarez FJ. Role of primary afferents in the developmental regulation of motor axon synapse numbers on Renshaw cells. *J Comp Neurol*. 2016;524(9):1892–919.
- Shin S, Kim TD, Jin F, van Deursen JM, Dehm SM, Tindall DJ, et al. Induction of prostatic intraepithelial neoplasia and modulation of androgen receptor by ETS variant 1/ETS-related protein 81. *Cancer Res*. 2009;69(20):8102–10.
- Shin S, Oh S, An S, Janknecht R. ETS variant 1 regulates matrix metalloproteinase-7 transcription in LNCaP prostate cancer cells. *Oncol Rep*. 2013;29(1):306–14.
- Morsalin S, Yang C, Fang J, Reddy S, Kayarthodi S, Childs E, et al. Molecular Mechanism of beta-Catenin Signaling Pathway Inactivation in ETV1-Positive Prostate Cancers. *J Pharm Sci Pharmacol*. 2015;2(3):208–16.
- Heeg S, Das KK, Reichert M, Bakir B, Takano S, Caspers J, et al. ETS-Transcription Factor ETV1 Regulates Stromal Expansion and Metastasis in Pancreatic Cancer. *Gastroenterology*. 2016;151(3):540–553 e514.
- Chi P, Chen Y, Zhang L, Guo X, Wongvipat J, Shamu T, et al. ETV1 is a lineage survival factor that cooperates with KIT in gastrointestinal stromal tumours. *Nature*. 2010;467(7317):849–53.
- Bradley CA, Salto-Tellez M, Laurent-Puig P, Bardelli A, Rolfo C, Tabernero J, et al. Targeting c-MET in gastrointestinal tumours: rationale, opportunities and challenges. *Nat Rev Clin Oncol*. 2017;14(9):562–76.
- Reddy KB, Nabha SM, Atanaskova N. Role of MAP kinase in tumor progression and invasion. *Cancer Metastasis Rev*. 2003;22(4):395–403.
- Schripsema J, de Rudder KE, van Vliet TB, Lankhorst PP, de Vroom E, Kijne JW, et al. Bacteriocin small of *Rhizobium leguminosarum* belongs to the class of N-acyl-L-homoserine lactone molecules, known as autoinducers and as quorum sensing co-transcription factors. *J Bacteriol*. 1996;178(2):366–71.
- Wang SW, Pan SL, Peng CY, Huang DY, Tsai AC, Chang YL, et al. CHM-1 inhibits hepatocyte growth factor-induced invasion of SK-Hep-1 human hepatocellular carcinoma cells by suppressing matrix metalloproteinase-9 expression. *Cancer Lett*. 2007;257(1):87–96.
- Liu WT, Jing YY, Yu GF, Chen H, Han ZP, Yu DD, et al. Hepatic stellate cell promoted hepatoma cell invasion via the HGF/c-Met signaling pathway regulated by p53. *Cell Cycle*. 2016;15(7):886–94.
- Ueki T, Fujimoto J, Suzuki T, Yamamoto H, Okamoto E. Expression of hepatocyte growth factor and its receptor c-met proto-oncogene in hepatocellular carcinoma. *Hepatology*. 1997;25(4):862–6.
- Ke AW, Shi GM, Zhou J, Wu FZ, Ding ZB, Hu MY, et al. Role of overexpression of CD151 and/or c-Met in predicting prognosis of hepatocellular carcinoma. *Hepatology*. 2009;49(2):491–503.
- Rhee H, Kim HY, Choi JH, Woo HG, Yoo JE, Nahm JH, et al. Keratin 19 Expression in Hepatocellular Carcinoma Is Regulated by Fibroblast-Derived HGF via a MET-ERK1/2-AP1 and SP1 Axis. *Cancer Res*. 2018;78(7):1619–31.
- Wang ZL, Liang P, Dong BW, Yu XL, Yu DJ. Prognostic factors and recurrence of small hepatocellular carcinoma after hepatic resection or microwave ablation: a retrospective study. *J Gastrointest Surg*. 2008;12(2):327–37.
- Monte D, Coutte L, Baert JL, Angeli I, Stehelin D, de Launoit Y. Molecular characterization of the ets-related human transcription factor ER81. *Oncogene*. 1995;11(4):771–9.
- Dawson JC, Serrels A, Stupack DG, Schlaepfer DD, Frame MC. Targeting FAK in anticancer combination therapies. *Nat Rev Cancer*. 2021;21(5):313–24.
- Zhou J, Yi Q, Tang L. The roles of nuclear focal adhesion kinase (FAK) on cancer: a focused review. *J Exp Clin Cancer Res*. 2019;38(1):250.
- Chen JS, Li HS, Huang JQ, Dong SH, Huang ZJ, Yi W, et al. MicroRNA-379-5p inhibits tumor invasion and metastasis by targeting FAK/AKT signaling in hepatocellular carcinoma. *Cancer Lett*. 2016;375(1):73–83.
- Comoglio PM, Trusolino L, Boccaccio C. Known and novel roles of the MET oncogene in cancer: a coherent approach to targeted therapy. *Nat Rev Cancer*. 2018;18(6):341–58.

36. Helmbacher F, Dessaud E, Arber S, deLapeyriere O, Henderson CE, Klein R, et al. Met signaling is required for recruitment of motor neurons to PEA3-positive motor pools. *Neuron*. 2003;39(5):767–77.
37. Kherrouche Z, Monte D, Werkmeister E, Stoven L, De Launoit Y, Cortot AB, et al. PEA3 transcription factors are downstream effectors of Met signaling involved in migration and invasiveness of Met-addicted tumor cells. *Mol Oncol*. 2015;9(9):1852–67.
38. Hanzawa M, Shindoh M, Higashino F, Yasuda M, Inoue N, Hida K, et al. Hepatocyte growth factor upregulates E1AF that induces oral squamous cell carcinoma cell invasion by activating matrix metalloproteinase genes. *Carcinogenesis*. 2000;21(6):1079–85.
39. Wang H, Rao B, Lou J, Li J, Liu Z, Li A, et al. The Function of the HGF/c-Met Axis in Hepatocellular Carcinoma. *Front Cell Dev Biol*. 2020;8:55.
40. Osada S, Kanematsu M, Imai H, Goshima S. Clinical significance of serum HGF and c-Met expression in tumor tissue for evaluation of properties and treatment of hepatocellular carcinoma. *Hepatogastroenterology*. 2008;55(82–83):544–9.
41. Fu J, Su X, Li Z, Deng L, Liu X, Feng X, et al. HGF/c-MET pathway in cancer: from molecular characterization to clinical evidence. *Oncogene*. 2021;40(28):4625–51.
42. Liu DL, Lu LL, Dong LL, Liu Y, Bian XY, Lian BF, et al. miR-17-5p and miR-20a-5p suppress postoperative metastasis of hepatocellular carcinoma via blocking HGF/ERBB3-NF-kappaB positive feedback loop. *Theranostics*. 2020;10(8):3668–83.
43. Lv PC, Jiang AQ, Zhang WM, Zhu HL. FAK inhibitors in Cancer, a patent review. *Expert Opin Ther Pat*. 2018;28(2):139–45.
44. Mathieu LN, Larkins E, Akinboro O, Roy P, Amatya AK, Fiero MH, et al. FDA Approval Summary: Capmatinib and Tepotinib for the Treatment of Metastatic NSCLC Harboring MET Exon 14 Skipping Mutations or Alterations. *Clin Cancer Res*. 2022;28(2):249–54.
45. Tomlins SA, Laxman B, Dhanasekaran SM, Helgeson BE, Cao X, Morris DS, et al. Distinct classes of chromosomal rearrangements create oncogenic ETS gene fusions in prostate cancer. *Nature*. 2007;448(7153):595–9.
46. Janknecht R. EWS-ETS oncoproteins: the linchpins of Ewing tumors. *Gene*. 2005;363:1–14.
47. Segales L, Juanpere N, Lorenzo M, Albergo-Gonzalez R, Fumado L, Cecchini L, et al. Strong cytoplasmic ETV1 expression has a negative impact on prostate cancer outcome. *Virchows Arch*. 2019;475(4):457–66.
48. Jomrich G, Maroske F, Stieger J, Preusser M, Ilhan-Mutlu A, Winkler D, et al. MK2 and ETV1 Are Prognostic Factors in Esophageal Adenocarcinomas. *J Cancer*. 2018;9(3):460–8.
49. Lunardi A, Varmeh S, Chen M, Taulli R, Guarnerio J, Ala U, et al. Suppression of CHK1 by ETS Family Members Promotes DNA Damage Response Bypass and Tumorigenesis. *Cancer Discov*. 2015;5(5):550–63.
50. Khatiwada P, Kannan A, Malla M, Dreier M, Shemshedini L. Androgen up-regulation of Twist1 gene expression is mediated by ETV1. *PeerJ*. 2020;8:e8921.
51. Li Z, Zhang L, Ma Z, Yang M, Tang J, Fu Y, et al. ETV1 induces epithelial to mesenchymal transition in human gastric cancer cells through the upregulation of Snail expression. *Oncol Rep*. 2013;30(6):2859–63.
52. Oh S, Shin S, Lightfoot SA, Janknecht R. 14-3-3 proteins modulate the ETS transcription factor ETV1 in prostate cancer. *Cancer Res*. 2013;73(16):5110–9.
53. Xu K, Zhang Q, Chen M, Li B, Wang N, Li C, et al. N(6)-methyladenosine modification regulates imatinib resistance of gastrointestinal stromal tumor by enhancing the expression of multidrug transporter MRP1. *Cancer Lett*. 2022;530:85–99.
54. Fujii T, Koshikawa K, Nomoto S, Okochi O, Kaneko T, Inoue S, et al. Focal adhesion kinase is overexpressed in hepatocellular carcinoma and can be served as an independent prognostic factor. *J Hepatol*. 2004;41(1):104–11.
55. Chen JS, Huang XH, Wang Q, Chen XL, Fu XH, Tan HX, et al. FAK is involved in invasion and metastasis of hepatocellular carcinoma. *Clin Exp Metastasis*. 2010;27(2):71–82.
56. Itoh S, Maeda T, Shimada M, Aishima S, Shirabe K, Tanaka S, et al. Role of expression of focal adhesion kinase in progression of hepatocellular carcinoma. *Clin Cancer Res*. 2004;10(8):2812–7.
57. Kaposi-Novak P, Lee JS, Gomez-Quiroz L, Coulouarn C, Factor VM, Thorgeirsson SS. Met-regulated expression signature defines a subset of human hepatocellular carcinomas with poor prognosis and aggressive phenotype. *J Clin Invest*. 2006;116(6):1582–95.
58. Yu Y, Peng XD, Qian XJ, Zhang KM, Huang X, Chen YH, et al. Fes1 phosphorylation by Met promotes mitochondrial fission and hepatocellular carcinoma metastasis. *Signal Transduct Target Ther*. 2021;6(1):401.
59. Ran L, Chen Y, Sher J, Wong EWP, Murphy D, Zhang JQ, et al. FOXF1 Defines the Core-Regulatory Circuitry in Gastrointestinal Stromal Tumor. *Cancer Discov*. 2018;8(2):234–51.
60. Vitari AC, Leong KG, Newton K, Yee C, O'Rourke K, Liu J, et al. COP1 is a tumour suppressor that causes degradation of ETS transcription factors. *Nature*. 2011;474(7351):403–6.
61. Simon-Carrasco L, Jimenez G, Barbacid M, Drosten M. The Capicua tumor suppressor: a gatekeeper of Ras signaling in development and cancer. *Cell Cycle*. 2018;17(6):702–11.
62. Wong D, Yip S. Making heads or tails - the emergence of capicua (CIC) as an important multifunctional tumour suppressor. *J Pathol*. 2020;250(5):532–40.
63. Bordignon P, Bottoni G, Xu X, Popescu AS, Truan Z, Guenova E, et al. Dualism of FGF and TGF-beta Signaling in Heterogeneous Cancer-Associated Fibroblast Activation with ETV1 as a Critical Determinant. *Cell Rep*. 2019;28(9):2358–2372 e2356.
64. Batzorig U, Wei PL, Wang W, Huang CY, Chang YJ. Glucose-Regulated Protein 94 Mediates the Proliferation and Metastasis through the Regulation of ETV1 and MAPK Pathway in Colorectal Cancer. *Int J Med Sci*. 2021;18(11):2251–61.
65. Wang S, Hwang EE, Guha R, O'Neill AF, Melong N, Veinotte CJ, et al. High-throughput Chemical Screening Identifies Focal Adhesion Kinase and Aurora Kinase B Inhibition as a Synergistic Treatment Combination in Ewing Sarcoma. *Clin Cancer Res*. 2019;25(14):4552–66.
66. Klaeger S, Heinzlmeir S, Wilhelm M, Polzer H, Vick B, Koenig PA, et al. The target landscape of clinical kinase drugs. *Science*. 2017;358(6367):eaan4368.
67. Romito I, Porru M, Braghini MR, Pompili L, Panera N, Crudele A, et al. Focal adhesion kinase inhibitor TAE226 combined with Sorafenib slows down hepatocellular carcinoma by multiple epigenetic effects. *J Exp Clin Cancer Res*. 2021;40(1):364.
68. Gerber DE, Camidge DR, Morgensztern D, Cetnar J, Kelly RJ, Ramalingam SS, et al. Phase 2 study of the focal adhesion kinase inhibitor defactinib (VS-6063) in previously treated advanced KRAS mutant non-small cell lung cancer. *Lung Cancer*. 2020;139:60–7.
69. Bouattour M, Raymond E, Qin S, Cheng AL, Stammberger U, Locatelli G, et al. Recent developments of c-Met as a therapeutic target in hepatocellular carcinoma. *Hepatology*. 2018;67(3):1132–49.
70. Baltshukat S, Engstler BS, Huang A, Hao HX, Tam A, Wang HQ, et al. Capmatinib (INC280) Is Active Against Models of Non-Small Cell Lung Cancer and Other Cancer Types with Defined Mechanisms of MET Activation. *Clin Cancer Res*. 2019;25(10):3164–75.

Publisher's Note

Springer Nature remains neutral with regard to jurisdictional claims in published maps and institutional affiliations.